Dalton Transactions

PAPER

View Article Online
View Journal | View Issue

Cite this: *Dalton Trans.*, 2019, **48**, 15896

Bi- and tridentate stannylphosphines and their coordination to low-valent platinum†‡

J. Jacobo Salazar-Díaz,[a] Miguel A. Muñoz-Hernández,[a,b] Ernesto Rufino-Felipe,[a] Marcos Flores-Alamo,[c] Alejandro Ramírez-Solís[d] and Virginia Montiel-Palma*[a,b]

Received 15th August 2019,
Accepted 19th September 2019

DOI: 10.1039/c9dt03317c

rsc.li/dalton

Semirigid bifunctional tin-substituted *o*-tolylphosphines of general formulae $[Ph_2P(o\text{-}C_6H_4CH_2)SnR_3]$ (R = Ph, **1**; R = Me, **2**) and $[\{Ph_2P(o\text{-}C_6H_4CH_2)\}_2SnPh_2]$ (**3**) were synthesized and isolated in good yields. The new compounds were fully characterized by single-crystal X-ray diffraction and multinuclear solution NMR spectroscopic techniques. The observed $J(^{119}Sn,^{31}P)$ values in solution NMR spectroscopy as well as the P···Sn distances in the solid state and DFT calculations (B3LYP) on compounds **1** and **3** do not support the existence of intramolecular P → Sn bond interactions in either of the three compounds. **1** and **2** reacted with stoichiometric amounts of tristriphenylphosphine platinum(0) $[Pt(PPh_3)_3]$ under toluene refluxing conditions leading to formation of Pt(II) distorted square-planar complexes $[Ph_2P(o\text{-}C_6H_4CH_2)Pt(SnR_3)(PPh_3)]$, (R = Ph, **4**; R = Me, **5**), each bearing a five-membered carbometallated ring resulting from Pt coordination to P and the benzylic C sp^3 atom of the ligand architecture rather than from activation of the terminal Sn–C carbon bonds of the phenyl or methyl substituents which would have rendered six-membered rings. Additionally, the fragment SnR_3 also binds to the metal centre disposing *cis* to the cyclometalated carbon atom and to the single remaining PPh_3. This carbometallation takes place affecting the integrity of the ligand skeleton. NBO calculations show the Sn fragment coordinates to the metal as X-type stannyl, SnR_3. The analogous reaction of $[Pt(PPh_3)_3]$ towards the stannyldiphosphine **3** leads to the quantitative formation of complex $[(Ph_2P\text{-}o\text{-}C_6H_4CH_2)Pt(Ph_2P\text{-}o\text{-}C_6H_4CH_2SnPh_3)]$, **6**, which exhibits five- and six-membered metallacycles at the expense of the ligand frame. All compounds were characterized exhaustively by solution spectroscopic measurements and by single crystal X-ray diffraction analysis. DFT computations corroborate the higher stability of the observed products over those resulting from preservation of the ligand backbone.

Introduction

Within the field of ligand design, incorporating strong σ-electron donors into the architecture of phosphine ligands often leads to enhanced electron density at the transition metal centre, in turn preparing the complex to undergo difficult transformations[1–4] or exhibiting catalytic activity.[5–10] Amongst the preferred designs, phosphines functionalized with Si occupy a privileged position.[11,12] In comparison, significantly less studies incorporating the heavier group 14 elements into phosphines have been performed.[13–17] Kameo and Nakazawa showed that in pentacoordinate trigonal bipyramidal rhodium complexes $[\{(Ph_2P)(C_6H_4)\}_3E\text{-}Rh(CO)]$ (where E = Si, Ge, Sn) derived of tetradentate EP_3-type ligands, the σ-electron donor ability and *trans* influence of the group 14 element E follows the trend Sn ~ Ge < Si.[3]

As an extension of our program targeting the reactivity of semirigid phosphine ligands functionalized with Si,[18–21] which makes use of the so-called "chelate assistance"[22,23] for the coordination of the group 14 element, we now report the synthesis of organotin substituted phosphines $[Ph_2P(o\text{-}C_6H_4CH_2)SnR_3]$ (R = Ph, **1**; R = Me, **2**) and $[\{Ph_2P(o\text{-}C_6H_4CH_2)\}_2SnPh_2]$ (**3**) and their coordination to platinum upon reaction towards tris(triphenylphosphine)plati-

[a]*Centro de Investigaciones Químicas-IICBA, Universidad Autónoma del Estado de Morelos, Av. Universidad 1001, Col. Chamilpa, Cuernavaca, Morelos 62209, Mexico. E-mail: vmontiel@chemistry.msstate.edu*
[b]*Department of Chemistry, Mississippi State University, Box 9573, Mississippi State, Mississippi 39762, USA*
[c]*Facultad de Química, Universidad Nacional Autónoma de México, Mexico City 04510, Mexico*
[d]*Centro de Investigación en Ciencias-IICBA, Universidad Autónoma del Estado de Morelos, Av. Universidad 1001, Col. Chamilpa, Cuernavaca, Morelos 62209, Mexico*

†VMP is delighted to dedicate Professor Robin N. Perutz this contribution in celebration of his 70th birthday. Robin, thank you for your teachings and for being an inspiration throughout my academic life.

‡Electronic supplementary information (ESI) available: NMR and IR spectra of all complexes, X-Ray diffraction data of complexes as well as theoretical calculations details and optimizations. Text files of all computed molecule Cartesian coordinates. CCDC 1909928–1909933 for **1–6**. For ESI and crystallographic data in CIF or other electronic format see DOI: 10.1039/c9dt03317c

num(0), [Pt(PPh$_3$)$_3$]. Herein we report the quantitative formation of complexes **4**, **5** and **6** with square planar coordination geometry about Pt, bearing five-membered metallacycle rings resulting selectively from the activation of Sn–C sp^3 of the benzylic carbons rather than of the terminal Sn–C sp^2 phenyl or Sn–C sp^3 methyl substituents which would have rendered six-membered metallacycles.

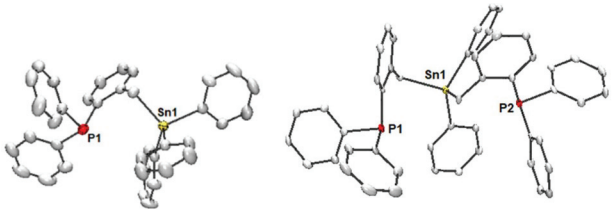

Fig. 1 ORTEP drawings of metalloligands **1** (left) and **3** (right) with ellipsoids at 30% probability level and hydrogen atoms omitted for clarity. Sn···P distances in Å for **1**: 3.917, for DFT-**3**: 3.999 and 3.975.

Results and discussion

Synthesis and characterization of triphenyl-(*o*-diphenylphosphinobenzyl)tin [Ph$_2$P(*o*-C$_6$H$_4$CH$_2$)SnPh$_3$], 1 and trimethyl-(*o*-diphenylphosphinobenzyl)tin [Ph$_2$P(*o*-C$_6$H$_4$CH$_2$)SnMe$_3$], 2

Compounds **1** and **2** were synthesized as shown in Scheme 1 from the organolithium phosphine [Ph$_2$P(*o*-C$_6$H$_4$CH$_2$Li·TMEDA)][24] adapting the method previously reported for the synthesis of *o*-tolyl-dimethylsilylphosphines.[19,25,26] Therefore, monolithiation of diphenyl-*o*-tolylphosphine in the presence of TMEDA and subsequent quenching with excess R$_3$SnCl led after work up to pure **1** and **2** in good yields (85% and 70% respectively, Scheme 1). Their full characterization is given in the experimental part and in ESI.‡ Herein, only the main features are discussed. Complexes **1** and **2** show in the ^{31}P NMR spectra signals at δ −16.0 and −14.5 with $^4J(^{119}\mathrm{Sn},^{31}\mathrm{P})$ = 37 Hz and 21 Hz respectively. Dative P → Sn interactions of different strengths leading to hypervalent species have been reported in phosphorus derivatives of Lewis acids including R$_2$P(CH$_2$)$_3$SnMe$_2$Cl[27] and rigid *ortho*-phenylene backbones R$_2$P(*o*-C$_6$H$_4$)SnClR′$_2$[28] and (Ph$_2$P-*o*-C$_6$H$_4$)$_3$SnF.[29] A significant dative interaction gives rise to metallacyle rings exhibiting modified chemical shifts in accordance with the increased coordination geometry and enlarged $J(^{119}\mathrm{Sn},^{31}\mathrm{P})$ coupling constants (>100 Hz).[27,28,30] The observed $J(^{119}\mathrm{Sn},^{31}\mathrm{P})$ values in both our compounds **1** and **2** do not support the presence of significant P → Sn interactions. Moreover, in the solid state the single crystal X-ray diffraction molecular structures of **1** and **2** (Fig. 1 and ESI‡) show central sp^3 hybridized Sn centres with close to ideal tetrahedral angles in **1**; while those around P are in line with a trigonal pyramidal geometry. The bond distances are also consistent with the other reported structures of organotin functionalized phosphines.[31,32] The P···Sn distances in **1** (3.917 Å) and **2** (two crystallographic independent molecules at 3.692 Å and 3.843 Å) are closer to the sum of the van der Waals radii[33] at 4.2 Å than to the sum of covalent radii, 2.75 Å.[34]

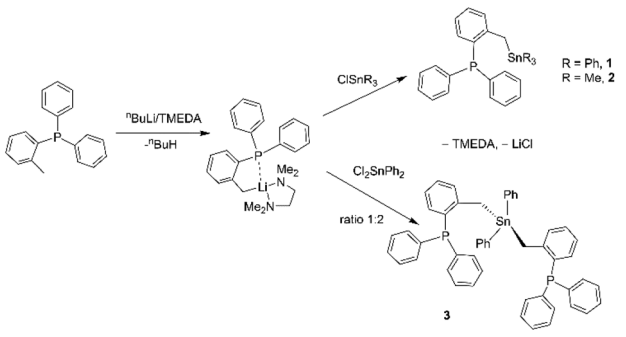

Scheme 1 Synthesis of bifunctional semirigid stannylphosphine ligands **1–3**.

Synthesis and characterization of diphenyl-bis-(*o*-diphenylphosphinobenzyl)tin [{Ph$_2$P(*o*-C$_6$H$_4$CH$_2$)}$_2$SnPh$_2$], 3

In analogous fashion, compound **3** was synthesized in good yield (80%) as a fine white powder from the reaction of two equivalents of lithium precursor [Ph$_2$P(*o*-C$_6$H$_4$CH$_2$Li·TMEDA)][24] with one equivalent of Ph$_2$SnCl$_2$ (Scheme 1). The formation of **3** is favoured over that of the monophosphine [Ph$_2$P(*o*-C$_6$H$_4$CH$_2$)SnPh$_2$Cl], which is not detected even if using a 1 : 1 stoichiometric ratio of the reagents. In solution, ^{1}H, ^{13}C{^{1}H}, ^{31}P{^{1}H}, and ^{119}Sn{^{1}H} NMR spectra show that the C_2 symmetry observed in the crystal structure is maintained (ESI‡). In the ^{31}P{^{1}H} and ^{119}Sn{^{1}H} NMR spectra, a singlet with Sn satellites and a triplet are respectively observed at δ −15.1 and −103.5, with a measured $^4J(^{119}\mathrm{Sn},^{31}\mathrm{P})$ = 34 Hz, which again does not back up a significant intramolecular P → Sn interaction in solution. The single crystal X-ray diffraction study of compound **3** gave a low-quality data set from which we obtained a refined structure consistent with the spectroscopic characterization. In view of this, we have not used it to discuss bond lengths and angles. Instead, we turned to a DFT model (Fig. 1 and ESI‡). The molecular structure shows a tetrahedral Sn atom and two phosphorous atoms in close to ideal trigonal pyramidal geometries. The P1···Sn and P2···Sn distances in compound **3** are 3.999 and 3.975 Å, longer than in **1** and **2** (X-ray diffraction) and far from those in compounds with a significant P → Sn dative interaction. In the closely related compound [{Ph$_2$P-*o*-C$_6$H$_4$}$_2$SnMe$_2$] in which a feeble P → Sn interaction was proposed, shorter P···Sn distances were determined (3.481 and 3.394 Å).[35] The P → Sn dative interaction is significantly more important in compound [{Ph$_2$P-*o*-C$_6$H$_4$}$_3$SnF].[29] This was not only manifested in shorter P1···Sn distances at 3.3660 Å (for each of the three P atoms) in the solid state but it was also corroborated by the use of DFT computations which showed that there are three dative lone pair interactions from the phosphorous atoms with a single σ*-antibonding Sn–F orbital.

Synthesis and characterization of κ^2-C,P-(*o*-tolyl)diphenylphosphine-triphenylphosphine-triphenylstannyl platinum(II) [$Ph_2P(o\text{-}C_6H_4CH_2)Pt(SnPh_3)(PPh_3)$], 4 and κ^2-C,P-(*o*-tolyl) diphenylphosphine-triphenylphosphine-trimethylstannyl platinum(II) [$Ph_2P(o\text{-}C_6H_4CH_2)Pt(SnMe_3)(PPh_3)$], 5

No reaction takes place at room temperature after prolonged vigorous stirring of toluene solutions of $[Pt(PPh_3)_3]$ and equimolar amounts of either compounds **1** or **2**. However, refluxing the reaction mixtures led after workup to isolation of white solids as well as to release of PPh_3. The platinum(II) complexes $[Ph_2P(o\text{-}C_6H_4CH_2)Pt(SnR_3)(PPh_3)]$ (R = Ph, **4**; R = Me, **5**) were isolated in moderate to good yields (73 and 70%, respectively). Their proposed formulations are supported by solution spectroscopic data as well as by FTIR, elemental analyses and single crystal X-ray diffraction. Complexes **4** and **5** result from the activation of Sn–C sp^3 bonds of the benzylic carbons rather than of the terminal Sn–C sp^2 phenyl bond (in **4**) or Sn–C sp^3 methyl bond (in **5**) of the proligands **1** or **2**. Overall the reactivity results in the selective formation of five-membered carbometallated rings stemming from bonding of the P atom and the benzylic carbon. No detectable amounts of the corresponding six-membered metallacycles were observed by spectroscopic means. These findings are very different from those obtained in the reaction of related silylphosphines bearing one or two Si–H fragments. For example, reaction of $[PhP(o\text{-}C_6H_4CH_2\text{-}SiMe_2H)_2]$[19] with $[Pt(PPh_3)_3]$ leads to the formation of a chelate bonded through P and two Si where the ligand skeleton is preserved.[20] Also the reaction of $[Ph_2P(o\text{-}C_6H_4CH_2)SiMe_2H]$ towards $[PtCl_2(cod)]$ in the presence of a base results in formation of six-membered rings from Si–H bond activation.[36]

In complexes **4** and **5**, the SnR_3 moiety also binds to the metal centre disposing *trans* to the P atom of the cyclometallated ring and *cis* to the single remaining PPh_3 (Scheme 2). The main solution ^1H NMR spectroscopic features of **4** and **5** comprise the benzylic CH_2 hydrogens as multiplets with Pt satellites with $^2J(^1H,^{195}Pt)$ = 55 Hz in both cases. **5** displays a doublet signal at δ 0.27, assigned to the methyl groups bound to Sn and shows both ^{195}Pt and $^{117/119}Sn$ satellites in accordance with their isotopic abundance from which $^2J(^1H,^{117/119}Sn)$ = 40 Hz and $^3J(^1H,^{195}Pt)$ = 10 Hz are determined. In the $^{13}C\{^1H\}$ NMR spectrum, **4** shows a doublet at δ 29.5 due to *trans* P coupling, $^2J(^{13}C,^{31}P)$ = 81 Hz with ^{195}Pt satellites from which $^1J(^{13}C,^{195}Pt)$ = 477 Hz is determined, while the corresponding spectrum of complex **5** shows a similarly shifted signal at δ 29.1 (d, $^2J(^{13}C,^{31}P)$ = 84 Hz) with $^1J(^{13}C,^{195}Pt)$ = 509 Hz. The ^{13}C–^{195}Pt coupling constants are direct gauges of the bond strength in solution,[37] indicating a slightly larger better C_{2s}–Pt_{6s} orbital overlap in **5**[38] than in **4**, which can be attributed to the higher σ-donor character of $SnMe_3$ than $SnPh_3$ rendering the Pt centre more electron rich. Similar coupling constant values $^1J(^{13}C,^{195}Pt)$ of 420 and 505 Hz for the benzylic carbons were respectively determined for the six-coordinate benzylic substituted stannylcarborane Pt(II) complexes [(bipy′)Pt$(C_6H_5)(CH_2C_6H_5)(t\text{-Bu-NC})(SnB_{11}H_{11})$] and [$Bu_3NMe$][(bipy′)Pt$(Br)(CH_2C_6H_5)(C_6H_5)(SnB_{11}H_{11})$] (where bipy′ = 4,4′-di-*t*-butyl-2,2′-bipyridine),[39] the first value being less similar to ours likely due to it belonging to a zwiterionnic species with a formally positive Pt centre. Additionally, complex **5** shows the signal due to the methyl carbons on the Sn atom as a doublet at δ −6.7, which is close to the resonance found for [$(Me_3SnCH_2CH_2Ph_2P)Pt(PPh_2CH_2CH_2SnMe_2)(Me)$] at δ −6.5.[22]

The $^{31}P\{^1H\}$ and $^{119}Sn\{^1H\}$ NMR spectroscopic data for the new complexes are summarized in Table 1. The $^{31}P\{^1H\}$ NMR spectra of complexes **4** and **5** show two similarly shifted doublet signals indicative of the *cis*-arrangement of the P nuclei (with $^2J(^{31}P,^{31}P)$ = 13 Hz in **4** and 11 Hz in **5**. Decoupling experiments allowed us to assign the signals at lowest field (δ 49.5, in **4** and **5**) as belonging to the P nuclei of the five-membered metallacycle which dispose *trans* to the SnR_3 moieties. The signals at highest field (δ 23.2, in **4** and δ 26.8 ppm, in **5**) are assigned to the remaining coordinated PPh_3, which resonates at a similar field than in other reported *trans* Sn–Pt–PPh_3 containing complexes including [$Cl_2Sn(\mu\text{-pyS})_2Pt(PPh_3)$] (where pyS = pyridine-2-thiolate) where PPh_3 appears at δ 24.3 in the ^{31}P NMR spectrum[40] and [$Os_3(CO)_9\{Pt(C_6H_5)(PPh_3)_2\}(\mu\text{-}SnPh_2)_2\text{-}(\mu_3\text{-SnPh})$] where *trans* PPh_3 appears at δ 34.8.[41] Moreover, for complex **4**, the value of the coupling constant $^1J(^{31}P,^{195}Pt)$ = 2388 Hz, determined from the Pt satellites of the signal at δ 49.5, is considerably larger than the corresponding one for **5** also at δ 49.5, which is $^1J(^{31}P,^{195}Pt)$ = 1978 Hz. Since it is generally stated that a stronger *trans* influence ligand will weaken the bond between the metal and the *trans* ligand,[42–44] a larger $^1J(^{31}P,^{195}Pt)$ value in complex **4** with respect to **5**, is in agreement with the higher *trans* influence of $SnMe_3$ with respect to $ShPh_3$. In addition, the values of the $^2J(^{31}P,^{119/117}Sn)$ coupling constants associated to the P atoms of the metallacycles are slightly larger for complex **4** ($^2J(^{31}P,^{119}Sn)$ = 1888 Hz and $^2J(^{31}P,^{117}Sn)$ = 1798 Hz) than for **5** ($^2J(^{31}P,^{119}Sn)$ = 1729 Hz and $^2J(^{31}P,^{117}Sn)$ = 1654 Hz). This behaviour has been previously studied by Lin and Marder in *trans*-[$ClPtL(PMe_3)_2$], predicted at the DFT level[45] and explained as the result of additive non-negligible *cis* influences.[43]

In the $^{119}Sn\{^1H\}$ spectra, multiplet signals are observed for both complexes: at δ 44.2 for **4** and at δ −15.6 for **5**. The spectrum of complex **4** is a higher order multiplet which approximates a doublet of doublets due to coupling to both inequivalent P nuclei. Complex **5** appears as a doublet of doublets. The coupling constants obtained are in line with the observations

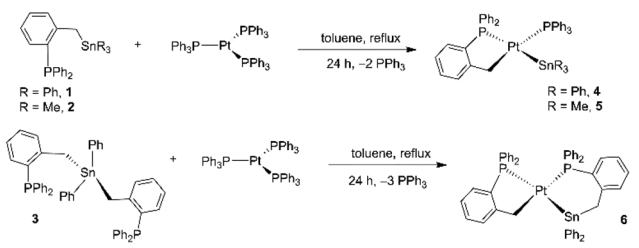

Scheme 2 The synthesis of complexes **4–6**.

Table 1 Relevant NMR spectroscopic data for complexes **4–6**

Complex	δ $^{31}P\{^1H\}$ $_{(PPh_3 \text{ or } 6MR^*)}$ [a] / ppm	$^{31}P\{^1H\}_{(5MR^{**})}$ [a] / ppm	$^{119}Sn\{^1H\}$ [b]
4	23.2 (d) $^2J(^{31}P,^{31}P)$ = 13 Hz $^1J(^{31}P,^{195}Pt)$ = 2183 Hz $^2J(^{31}P,^{117,119}Sn)$ = 177 Hz	49.5 (d) $^2J(^{31}P,^{31}P)$ = 13 Hz $^1J(^{31}P,^{195}Pt)$ = 2388 Hz $^2J(^{31}P,^{119}Sn)$ = 1888 Hz $^2J(^{31}P,^{117}Sn)$ = 1798 Hz	−44.2 (m) $^2J(^{119}Sn,^{31}P_{cis})$ = 184 Hz $^2J(^{119}Sn,^{31}P_{trans})$ = 1885 Hz $^1J(^{119}Sn,^{195}Pt)$ = 12 080 Hz
5	26.8 (d) $^2J(^{31}P,^{31}P)$ = 11 Hz $^1J(^{31}P,^{195}Pt)$ = 2238 Hz $^2J(^{31}P,^{117,119}Sn)$ = 170 Hz	49.5 (d) $^2J(^{31}P,^{31}P)$ = 11 Hz $^1J(^{31}P,^{195}Pt)$ = 1978 Hz $^2J(^{31}P,^{119}Sn)$ = 1729 Hz $^2J(^{31}P,^{117}Sn)$ = 1654 Hz	−15.6 (dd) $^2J(^{119}Sn,^{31}P_{cis})$ = 172 Hz $^2J(^{119}Sn,^{31}P_{trans})$ = 1730 Hz $^1J(^{119}Sn,^{195}Pt)$ = 10 945 Hz
6	17.0 (d) $^2J(^{31}P,^{31}P)$ = 13 Hz $^1J(^{31}P,^{195}Pt)$ = 1978 Hz $^2J(^{31}P,^{117,119}Sn)$ = 225 Hz	50.4 (d) $^2J(^{31}P,^{31}P)$ = 13 Hz $^1J(^{31}P,^{195}Pt)$ = 2328 Hz $^2J(^{31}P,^{119}Sn)$ = 1807 Hz $^2J(^{31}P,^{117}Sn)$ = 1726 Hz	71.2 (dd) $^2J(^{119}Sn,^{31}P_{cis})$ = 215 Hz $^2J(^{119}Sn,^{31}P_{trans})$ = 1807 Hz $^1J(^{119}Sn,^{195}Pt)$ = 11 923 Hz

[a] $*_{6MR}$ = six-membered ring. 161 MHz, $C6D_6$. [b] $**_{5MR}$ = five-membered ring. 149 MHz, C_6D_6.

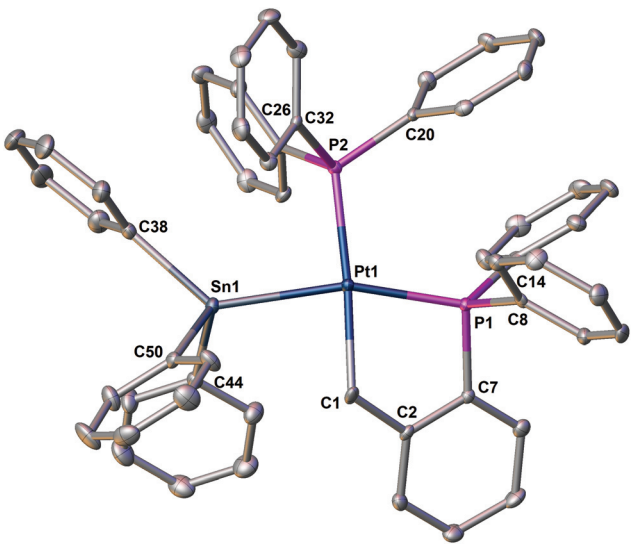

Fig. 2 ORTEP drawing of complex **4** with ellipsoids at 30% probability level. Selected bond lengths in Å, and angles in degrees: Pt1–C1 2.128(5), Pt1–P1 2.2822(17), Pt1–P2 2.2791(14), Pt1–Sn1 2.6036(5); C1–Pt1–P1 80.27(18); C1–Pt1–P2 175.04(19), C1–Pt1–Sn1 84.46(17), P1–Pt1–Sn1 160.19(4), P2–Pt1–Sn1 91.71(4), P2–Pt1–P1 104.14(5). For some comparisons, in **5**: Pt1–C1 2.120(4), Pt1–P1 2.2850(11), Pt1–P2 2.2775(11), Pt1–Sn1 2.6026(3).

in ^{31}P NMR spectroscopy and overall larger for complex **4** than for complex **5**.[46]

Additionally, crystals of **4** and **5** suitable for their study by single crystal X-ray diffraction were obtained. Fig. 2 shows the molecular structure of **4** while that of **5** and other important crystallographic information are gathered in ESI.‡ The Pt centres are tetracoordinated with distorted square planar geometry exhibiting *cis* angles around Pt between 80.27(18)–104.14(5)° in **4** and 81.49(12)–102.62(4)° in **5**,§ reflecting the distortion imposed by the bidentate $\{Ph_2P(o\text{-}C_6H_4CH_2)\}$ moiety. The distances determined by X-ray diffraction for **4** and **5** are very similar and do not allow us to draw meaningful conclusions on the comparative *trans* influences of $SnMe_3$ *versus* $SnPh_3$ in the solid state (ESI‡). The data are in agreement with retention of the structure in both solid and solution states.

Synthesis and characterization of κ^2-C,P-[(*o*-benzyl)diphenylphosphine]-κ^2-P,Sn-[(*o*-benzyldiphenylstannyl)diphenylphosphine] platinum(II) [$(Ph_2P\text{-}o\text{-}C_6H_4CH_2)Pt(Ph_2P\text{-}o\text{-}C_6H_4CH_2SnPh_3)$], 6

In analogous fashion to the synthesis of **4** and **5**, prolonged reflux (24 h) of an equimolar toluene mixture of $[Pt(PPh_3)_3]$ and **3** led after workup to isolation of a light yellow solid. Complex $[(Ph_2P(o\text{-}C_6H_4CH_2)Pt(Ph_2P(o\text{-}C_6H_4CH_2SnPh_3)]$, **6** was isolated in good yield (70%) (Scheme 2). Its formulation is supported by solution spectroscopic data as well as by FTIR, elemental analyses and single crystal X-ray diffraction. Ligand **3** also undergoes cleavage of the benzylic CH_2–Sn bond upon coordination to Pt, resulting also in the formation of a five-membered carbometallated ring from coordination of one of the P atoms and the benzylic carbon. The remaining phosphorous atom of proligand **3** also coordinates to Pt as does the Sn atom, now forming a six-membered metallacycle ring. As in complexes **4** and **5**, the Sn group binds *trans* to the P atom of the five-membered ring and the two P atoms arrange *cis* to one another, thus attaining a similar structure (Scheme 2). The main solution spectroscopic features of **6** comprise in the ^1H NMR solution spectrum, a multiplet signal at δ 4.52 with ^{195}Pt

§ Two crystallographically independent molecules were found in the unit cell of **5**. Herein selected details of one of them are given, the complete information is gathered in ESI.†

satellites indicating a $^2J(^1H,^{195}Pt)$ = 50 Hz due to the hydrogens directly attached to the carbometallated carbon, as well as a very broad signal ($w_{1/2}$ = 21 Hz) at δ 2.62 assigned to the methylene hydrogens bound to Sn. In the $^{13}C\{^1H\}$ NMR spectrum, two doublet signals for methylene carbons are observed at δ 22.0 and 21.6 ppm. The pseudotriplet at δ 22.0 is assigned to the CH_2 carbon nuclei of the six-membered metallacycle ring based on the lower value for its coupling constant to Pt, $^2J(^{13}C,^{195}Pt)$ = 23 Hz and observable $^1J(^{13}C–^{119}Sn)$ = 37 Hz. In comparison, the doublet at 21.6 allows to measure a much larger coupling constant to Pt $^1J(^{13}C,^{195}Pt)$ = 488 Hz and the observation of a *trans* $^2J(^{13}C,^{31}P)$ = 81 Hz, and is assigned to the methylene carbon of the five-membered metallacycle ring with a direct Pt–C bond.

The $^{31}P\{^1H\}$ and $^{119}Sn\{^1H\}$ NMR spectral data for **6** are also summarized in Table 1. In the $^{31}P\{^1H\}$ NMR spectra the lowest field signal at $\delta \approx 50$ is assigned to the P atom of the five-membered metallacycle ring, it shows two sets of Sn satellites with the predicted intensity which thanks to the ^{119}Sn experiments are assigned as $^2J(^{31}P,^{119}Sn)$ = 1807 Hz and $^2J(^{31}P,^{117}Sn)$ = 1726 Hz. Additionally, the observation of the ^{195}Pt satellites allow the determination of $^1J(^{31}P,^{195}Pt)$ = 2328 Hz. Despite this coupling constant being rather similar to that observed in complex **4**, it is slightly reduced, indicating that the Sn moiety forming part of the chelate ring, $SnPh_2CH_2(o\text{-}C_6H_4)PPh_2$, exerts a marginally more important *trans* influence than $SnPh_3$. From the satellites of the highest field signal shifted to δ 17.0 for **6**, the determination of $^2J(^{31}P,^{119}Sn)$ = 225 Hz and $^2J(^{31}P,^{117}Sn)$ = 199 Hz as well as $^1J(^{31}P,^{195}Pt)$ = 1978 Hz was possible. In complex **6**, the value of the $^1J(^{31}P,^{195}Pt)$ for the five-membered P moiety is smaller (17%) than the corresponding for the six-membered ring. This behaviour can be ascribed to different *trans* influences likely coupled with steric effects. In general $^2J(^{31}P,^{119,117}Sn)$ and $^1J(^{31}P,^{195}Pt)$ fall in the range found for other platinum complexes that incorporate stannyl moieties.[47] Finally, the coupling constants obtained from the $^{119}Sn\{^1H\}$ NMR spectrum of complex **6** are similar to those of complexes **4** and **5**.

The solid-state molecular structure of complex **6** shown in Fig. 3 confirms the *cis* disposition of the two phosphorous atoms coordinated to Pt forming two metallacycle rings: a five-membered one in which a P and a benzylic CH_2 coordinate as in complexes **4** and **5**; and a six-membered ring originating from the coordination of P and Sn. Once again, the data agree with the same molecular structure in solution and solid state.

DFT computations

The DFT structures of PPh_3 and ligands **1**, and **3**, and complexes **4**, **4B**, **6**, **6B**, and $[Pt(PPh_3)_3]$ (Scheme 2 and Fig. 4) were computed *in vacuo* and in toluene using the Polarizable Continuum Model (PCM) at the B3LYP level of theory with a mixed basis set as detailed in the Experimental section. Table S9 (ESI‡) gathers the computed Gibbs free energy values of the optimized structures. The optimizations were also carried out for the non-observable six-membered ring chelates **4B** and **6B** (Fig. 4) in which the ligand backbone is

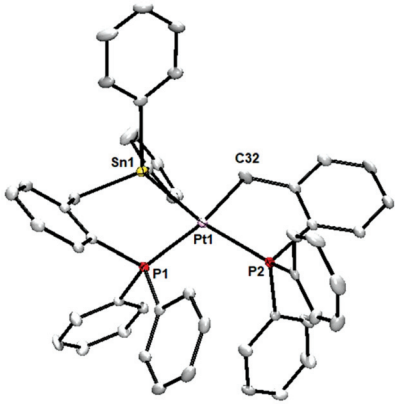

Fig. 3 ORTEP drawing of complex **6** with ellipsoids at 30% probability level. Selected bond lengths in Å, and angles in degrees: Pt1–Sn1 2.5693(4), Pt1–P1 2.3007(11), Pt1–P2 2.3060(11), Pt1–C32 2.115(5); P1–Pt1–Sn1 87.79(3), P2–Pt1–Sn1 164.48(3), C32–Pt1–Sn1 82.23(15), C19–Sn1–Pt1 110.03(13).

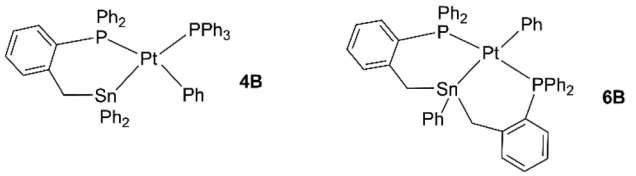

Fig. 4 The structures of the computed experimentally unobservable chelate complexes **4B** and **6B** resulting from formation of six-membered rings with preservation of the ligand structure.

preserved and were initially expected to be formed. The $\Delta G_{298\ K}$ values reflect that reactions that give complexes **4** and **6** are thermodynamically more favourable than reactions that afford complexes **4B** and **6B** in the investigated experimental conditions. $\Delta H_{298\ K}$ values for complexes **4** and **4B**, and **6** and **6B** are also consistent with experimental results, being **4** more stable by 5.18 kcal mol^{-1} than **4B**, and **6** by 12.69 kcal mol^{-1} than **6B**. It might be hypothesized that initial *trans* coordination of the P ligands around Pt would lead to the formation of a ten-membered ring[48] which will subsequently be followed by intramolecular activation of the Sn–C sp^3 bond to render a more stable five-membered metallacycle. We turned to NBO analysis to gain insight into the nature of the Pt–Sn bond in complexes **4**, **4B**, **6** and **6B**. Natural electronic population analyses show a proportional filling of 5s and 5p orbitals of tin atoms for complexes **4**, **4B**, **6** and **6B** (5s 52–54%; 5p 47–45%), in accordance to tetravalent tin. It has been reported, both formal tin(III) and tin(IV)[40] compounds may possess these tetravalent tin characteristics, depending on the nature of the Sn–Pt bond (Sn(III)–Pt(I) *versus* Sn(IV)–Pt(0)). Our results show essentially apolar Pt–Sn bonds in which the platinum contribution ranges from 46–58% and the tin contribution from 42–54%. The same analysis rendered polar Pt–C bonds (platinum contribution 0–40%, carbon contribution 60–100%), therefore the Sn ligand can be described formally as Sn(III)

bound to Pt(I). These findings are very similar to those in the complexes [MeSn(μ-2-$C_6F_4PPh_2$)$_2$Pd(κ-C-2-$C_6F_4PPh_2$)], [Me_2Sn(μ-2-$C_6F_4PPh_2$)Pd(κ^2-2-$C_6F_4PPh_2$)] and [MeSn(μ-2-$C_6F_4PPh_2$)$_2$PdCl].[49]

Atomic Natural charges on model compound $Me_2Sn(C_6H_5)(CH_2C_6H_5)$ confirmed that the polarity of the Sn–C bonds follows the trend: Sn–C (methyl) < Sn–C (phenyl) < Sn–C (benzyl) (see ESI‡). However, Natural bond analysis of the three types of bonds does not show any significant differences for the atomic contribution (ESI‡). To further discuss the selective access to complexes **4** and **6** and the lack of formation of **4B** and **6B**, a discussion on E–C bond activation is pertinent. To our knowledge, the selectivity of Sn–C sp^3 *versus* Sn–C sp^2 bond activation has been sparingly mentioned.[50,51] In contrast, the related C–C and Si–C bonds cleavages have been extensively investigated. Milstein and other workers studied the selectivity of unstrained C sp^3–C sp^3 *versus* C sp^3–C sp^2 activations, finding the product of the latter cleavage to be more stable than the former due to the high stability of the M–C sp^2 bond.[52,53] Love showed that the selectivity of the C–C reductive elimination in a Pt(IV) system is driven not only by the hybridization of the hydrocarbyl substituents but also by the coordination geometry and flexibility of the ligand scaffold.[54] Si–C activations by transition metals have been considerably less studied. Turculet[55] and Iwasawa[56] reported Si–C sp^3 cleavages induced by the chelate effect in Pd systems. Kameo and Nakazawa notably reported a systematic comparison on the Si–C sp^3 *versus* Si–C sp^2 activations in Rh and Ir systems concluding that both proceeded with a significant rate when employing the methylphenyl substituted ligand [*o*-{Ph_2P-C_6H_4}$_2$SiMePh], the selectivity being strongly dependent upon the temperature of reaction due to Si–C sp$^3_{(Me)}$ cleavage being entropically favoured but enthalpically unfavoured in comparison with Si–C sp$^2_{(Ph)}$.[57] Thus in the present case, the fact that reactions take place only at elevated temperatures in contrast with the reactions of other Pt precursors with Sn sources which occur at lower temperature[46] coupled with higher stability of five-membered cyclometalated[58] rings in comparison with six-membered; leads to complete selectivity of the Sn–C sp^3 bond cleavage over Si–C sp^2 in complexes **4** and **6**. The argument of the metallacycle ring size can also be employed to explain the formation of **5**.[59] It has been previously stated the possible role of steric hindrance in the methyl *versus* phenyl activation,[57] this is not relevant in the present case.

We are currently investigating the catalytic activity of the Pt complexes in cooperative Friedel–Crafts alkylation of aromatics,[60,61] the results of which will be reported in due course.

Experimental section

All experiments were performed under argon atmosphere using standard Schlenk methods or in an MBraun glove box. All solvents were either dried and distilled from appropriate drying agent or purified over a MBraun column system. In either case, they were degassed prior to use. Benzene-d_6 was degassed *via* three freeze–pump–thaw cycles and stored over molecular sieves in an ampoule fitted with a J. Young's valve. Deuterated solvents, *n*BuLi (2.5 M in hexane), Ph_3SnCl, Ph_2SnCl_2, Me_3SnCl were used as supplied for the respective provider. Diphenyl *o*-tolyl phosphine and [Pt(PPh_3)$_3$] were synthetized according to reported procedures. Nuclear magnetic resonance was recorded on Varian Inova 400 MHz (9.4 T) and Varian VNMRS 700 MHz (16.45 T) and Bruker 500 MHz (AVIII-HD); the chemical shifts are given in units of ppm, with coupling constants in Hz. Infrared spectroscopy was carried out using a NICOLET 6700 spectroscope. Mass Spectrometry was carried out using a JMS700–JEOL spectrometer of high resolution.

Synthesis of triphenyl-(*o*-diphenylphosphinobenzyl)tin [$Ph_2P(o\text{-}C_6H_4CH_2)SnPh_3$], (1)

In a Schlenk flask, diphenyl-*o*-tolyl phosphine (1.00 g, 3.62 mmol) and TMEDA (0.54 mL, 3.60 mmol) were dissolved in 100 mL of hexane. A 2.5 M *n*BuLi solution in hexanes (1.6 mL, 4 mmol) was added by syringe at 273 K and the reaction mixture left to reach room temperature. Stirring was continued for 24 h, after which the *in situ* generated ([$Ph_2P(o\text{-}C_6H_4\text{-}CH_2Li\cdot TMEDA)$] was reacted with a solution of Ph_3SnCl (1.39 g, 3.61 mmol) in 20 mL hexane, added *via* cannula at room temperature. Stirring was continued for further 48 h after which a white precipitate was observed. The mixture was filtered-off and the solid residue re-dissolved in THF (15 mL) before being passed through a fritted glass filter and finally dried under vacuum to afford a fine white powder (yield 85%, m.p. 375 K). Crystals suitable for X-ray diffraction were obtained from a THF/hexane solution. Anal. Calcd for $C_{37}H_{31}PSn\cdot C_4H_8O$: C, 70.61; H, 5.64. Found C, 69.70; H, 4.98. ^{1}H NMR (700 MHz, C_6D_6): δ 7.50 (6H, dd, $^3J_{H-H}$ = 2.8 Hz, $^3J_{H-Sn}$ = 42.7 Hz sat), 7.18–7.15 (11H, m), 7.08–6.99 (9H, m), 6.93 (1H, t, $^3J_{H-H}$ = 7.3 Hz), 6.83 (1H, t, $^3J_{H-H}$ = 5.9 Hz), 6.76 (1H, t, $^3J_{H-H}$ = 7.3 Hz), 2.99 (2H, $^4J_{H-31P}$ = 7 Hz, $^2J_{H-119Sn/117Sn}$ = 70 Hz sat). ^{13}C{^{1}H} NMR (176 MHz, C_6D_6): δ 146.19 (d, $^1J_{13C-31P}$ = 25 Hz, C_{ipso}), 140.19 (d, $^5J_{13C-31P}$ = 3 Hz, $^1J_{13C-119Sn}$ = 491 Hz sat, $^1J_{13C-117Sn}$ = 481 Hz sat, C_{ipso}), 137.60 (s, $^2J_{13C-119Sn}$ = 35 Hz sat, CH_{arom}), 136.49 (d, $^1J_{13C-31P}$ = 9 Hz), 134.32 (CH_{arom}, d, $^2J_{13C-31P}$ = 19 Hz, C_{ipso}), 133.82 (s, CH_{arom}), 133.76 (d, $^2J_{13C-31P}$ = 6 Hz, C_{ipso}), 129.50 (s, CH_{arom}), 129.05 (s, $^3J_{13C-119Sn}$ = 10.5 Hz sat, CH_{arom}), 128.86 (d, $^2J_{13C-31P}$ = 12 Hz, CH_{arom}), 128.84 (s, $^2J_{13C-119Sn}$ = 49 Hz sat, CH_{arom}), 128.79 (s, CH_{arom}), 128.35 (s, CH_{arom}), 125.01 (s, $^5J_{13C-119Sn}$ = 17.5 Hz sat, CH_{arom}), 22.20 (d, $^4J_{13C-31P}$ = 27 Hz, $^1J_{13C-119Sn}$ = 331 Hz sat, $^1J_{13C-117Sn}$ = 318 Hz sat, CH_2). ^{31}P{^{1}H} NMR (161 MHz, C_6D_6) δ: −16.00 (s, $^4J_{31P-119Sn}$ = 37 Hz sat). ^{119}Sn{^{1}H} NMR (149 MHz, C_6D_6) δ: −112.70 (d, $^4J_{119Sn-31P}$ = 37 Hz). MS (EI+) 626 *m*/*z* $[M-1]^+$.

Synthesis of trimethyl-(*o*-diphenylphosphinobenzyl)tin [$Ph_2P(o\text{-}C_6H_4CH_2)SnMe_3$], (2)

Compound **2** was synthesized and purified in a similar manner to **1**, by preparing [$Ph_2P(o\text{-}C_6H_4\text{-}CH_2Li\cdot TMEDA)$] (3.62 mmol) and *in situ* reacting it with a hexane solution of

Me_3SnCl (721 mg, 3.62 mmol) in the same reaction conditions. A transparent waxy solid was obtained in 70% isolated yield. Crystals suitable for X-ray diffraction were obtained from a THF/hexane solution. Anal. Calcd for $C_{22}H_{25}PSn$: C, 60.17; H, 5.74. Found C, 59.89; H, 5.81. ^{1}H NMR (500 MHz, C_6D_6) δ: 7.3–7.4 (m, 3H), 7.0 (m, 10H), 6.9 (m, 1H), 2.5 (2H, d, $^4J_{1H-31P}$ = 3 Hz, $^2J_{1H-119Sn}$ = 63.2 Hz sat) 0.17 (9H, s, $^2J_{1H-119Sn}$ = 52 Hz sat). $^{13}C\{^1H\}$ NMR (125.7 MHz, C_6D_6): δ 148.39(C_{ipso}, d, $^1J_{13C-31P}$ = 25.1 Hz), 137.13 (C_{ipso}, d, $^1J_{13C-31P}$ = 10 Hz), 134.41 (CH_{arom}, d $^1J_{13C-31P}$ = 20.1 Hz) 133.62 (CH_{arom}, s, $^1J_{13C-119Sn}$ = 12.6 Hz sat), 133.15 (C_{ipso}, d, $^1J_{13C-31P}$ = 8.8 Hz), 129.32 (CH_{arom}, d, $^1J_{13C-31P}$ = 8.8 Hz), 128.94 (CH_{arom}, s, $^1J_{13C-119Sn}$ = 13.8 Hz sat), 128.44 (C–H_{arom}, d, $^1J_{13C-31P}$ = 7.5 Hz), 128.35 (CH_{arom}, d, $^1J_{13C-31P}$ = 6.2 Hz), 124.31 (CH_{arom}, s, $^1J_{13C-119Sn}$ = 13.8 Hz sat), 21.61 (CH_2, d, $^3J_{13C-31P}$ = 23.8 Hz), −8.25 (CH_3, d, $^5J_{13C-13P}$ = 5 Hz, $^1J_{13C-119Sn}$ = 325.1 Hz sat). $^{31}P\{^1H\}$ NMR (161.9 MHz, C_6D_6): δ −14.5 (s, $^4J_{31P-119Sn}$ = 21 Hz sat). $^{119}Sn\{^1H\}$ NMR (186.5 MHz, C_6D_6): δ 0.73 (s, $^4J_{119Sn-31P}$ = 22.3 Hz).

Synthesis of diphenyl-bis-(*o*-diphenylphosphinobenzyl)tin [{$Ph_2P(o\text{-}C_6H_4CH_2)$}$_2SnPh_2$], (3)

Complex **3** was synthesized and purified in a similar manner to **1**, by quenching [$Ph_2P(o\text{-}C_6H_4\text{-}CH_2Li\cdot TMEDA$)] (3.62 mmol) generated *in situ* with Ph_2SnCl_2 (622 mg, 1.81 mmol) in hexane (10 mL). The resulting white fine powder was obtained in good yield (80%). Crystals suitable for X-ray diffraction were obtained from a THF/hexane solution. Anal. Calcd for $C_{50}H_{42}P_2Sn\cdot C_4H_8O$: C, 72.42; H, 5.63. Found C, 71.99; H, 5.23. ^{1}H NMR (400 MHz, C_6D_6, 293 K): δ 7.52 (4H, m, $^3J_{1H-119Sn}$ = 43.6 Hz sat), 7.17 (6H, m, $^3J_{1H-1H}$ = 1.6 Hz) 7.11 6.97 (22H, m), 6.91–6.77 (6H, m), 3.06 (4H, d, $^4J_{1H-31P}$ = 4.8 Hz, $^2J_{1H-119Sn}$ = 65 Hz sat). $^{13}C\{^1H\}$ NMR (100 MHz, C_6D_6): δ 146.83 (C_{ipso}, d, $^1J_{13C-31P}$ = 26 Hz), 142.3 (C_{ipso}, pseudot, $^5J_{13C-31P}$ = 8 Hz), 137.38 (CH_{arom}, s, $^2J_{13C-119Sn}$ = 33 Hz sat), 136.64 (4C_{ipso}, d, $^1J_{13C-31P}$ = 10 Hz), 134.39 (CH_{arom}, d, $^2J_{13C-31P}$ = 19 Hz), 133.91 (CH_{arom}, d, $^3J_{13C-31P}$ = 9 Hz), 133.57 (C_{ipso}, s, $^2J_{13C-119Sn}$ = 14.1 Hz sat), 129.38 (CH_{arom}, s, $^3J_{13C-119Sn}$ = 13 Hz sat), 128.82 (CH_{arom}, s), 128.76 (CH_{arom}, s), 128.58 (CH_{arom}, d, $^2J_{13C-31P}$ = 10 Hz), 128.53 (CH_{arom}, s), 128.50 (CH_{arom}, s), 124.79 (2CH_{arom}, s), 23.43 (CH_2, dd, $^5J_{13C-31P}$ = 7 Hz, $^3J_{13C-31P}$ = 25 Hz). $^{31}P\{^1H\}$ NMR (161 MHz, C_6D_6, 298 K): δ −15.11 (s, $^4J_{31P-119Sn}$ = 34 Hz sat). ^{119}Sn $\{^1H\}$ NMR (149 MHz, C_6D_6): δ −103.54 (t, $^4J_{119Sn-31P}$ = 34 Hz). MS (EI^+) 823 m/z $[M-1]^+$.

Synthesis of κ^2-C,P-(*o*-tolyl)diphenylphosphine-triphenylphosphine-triphenylstannyl platinum(II) [$Ph_2P(o\text{-}C_6H_4CH_2)Pt(SnPh_3)(PPh_3)$], (4)

In a Schlenk flask, [$Pt(PPh_3)_3$] (100 mg, 0.10 mmol) and compound **1** (64 mg, 0.10 mmol) in 20 mL toluene were refluxed for 24 h, after which time the red-orange solution showed a white precipitate. The red solution was filtered off and the white powder washed three times with cold hexane. The solid was dried under vacuum. Crystals suitable for X-ray diffraction analysis were grown from a THF/CH_2Cl_2 mixture. Yield 73%. Anal. Calcd for $C_{55}H_{46}P_2PtSn\cdot CH_2Cl_2$: C, 57.60; H, 4.14. Found: C, 57.28; H, 4.69. ^{1}H NMR (700 MHz, $CDCl_3$, 298 K) δ: 7.66 (1H, dd, $^3J_{H-H}$ = 7.7 Hz), 7.54 (1H, t, $^3J_{H-H}$ = 7.3 Hz), 7.46 (1H, t, $^3J_{H-H}$ = 6.6 Hz), 7.30 (2H, t, $^3J_{H-H}$ = 7.3 Hz), 7.20–7.12 (24H, m), 7.07 (3H, t, $^3J_{H-H}$ = 7.3 Hz), 6.99 (6H, t, $^3J_{H-H}$ = 7.3 Hz), 6.93 (6H, t, $^3J_{H-H}$ = 7.7 Hz), 3.85 (2H, m, $^2J_{H-H}$ = 2.4 Hz, $^3J_{H-31P}$ = 6.8 Hz, $^2J_{1H-195Pt}$ = 55.1 Hz). $^{13}C\{^1H\}$ NMR (176 MHz, C_6D_6, 298 K) δ: 160.72 (C_{ipso}, d, $^1J_{13C-31P}$ = 42 Hz, $^2J_{13C-195Pt}$ = 145 Hz), 147.64 (C_{ipso}, d, $^3J_{13C-31P}$ = 10 Hz, $^2J_{13C-195Pt}$ = 75 Hz, $^1J_{13C-119Sn}$ = 238 Hz), 138.05 (CH_{arom}, s, $^2J_{13C-119Sn}$ = 35.2 Hz), 135.78 (C_{ipso}, d, $^1J_{13C-31P}$ = 49.3 Hz), 134.29 (CH_{arom}, d, $^2J_{13C-31P}$ = 12.3 Hz), 132.9 (CH_{arom}, d, $^2J_{13C-31P}$ = 12.3 Hz), 132.48 (C_{ipso}, d, $^2J_{13C-31P}$ = 12.3 Hz), 132.15 (CH_{arom}, d, $^3J_{13C-31P}$ = 9 Hz), 131.93 (CH_{arom}, d, $^2J_{13C-31P}$ = 21 Hz), 130.93 (CH_{arom}, s), 129.89 (CH_{arom}, s), 129.54 (CH_{arom}, s), 128.57 (C_{ipso}, d, $^1J_{13C-31P}$ = 12.3 Hz), 128.35 (CH_{arom}, d, $^3J_{13C-31P}$ = 10 Hz), 127.10 (CH_{arom}, s, $^3J_{13C-119Sn}$ = 35 Hz), 126.29 (CH_{arom}, s), 125.01 (CH_{arom}, d, $^3J_{13C-31P}$ = 5 Hz), 28.64 (CH_2, d, $^2J_{13C-31P}$ = 81 Hz, $^1J_{13C-195Pt}$ = 477 Hz) ^{31}P $\{^1H\}$ NMR (161 MHz, C_6D_6, 298 K) δ: 49.5 (d, $^2J_{31P-31P}$ = 13 Hz, $^1J_{31P-195Pt}$ = 2388 Hz sat, $^2J_{31P-119Sn}$ = 1888 Hz sat, $^2J_{31P-117Sn}$ = 1798 Hz sat), 23.23 (d, $^2J_{31P-31P}$ = 13 Hz, $^1J_{31P-195Pt}$ = 2183 Hz sat, $^2J_{31P-119Sn}$ = 177 Hz sat). $^{119}Sn\{^1H\}$ RMN (149 MHz, C_6D_6, 298 K) δ: −44.2 (dd, $^2J_{119Sn-31Pcis}$ = 184 Hz, $^2J_{119Sn-31Ptrans}$ = 1885 Hz, $^1J_{119Sn-195Pt}$ = 12 080 Hz sat).

Synthesis of κ^2-C,P-(*o*-tolyl)diphenylphosphine-triphenylphosphine-trimethylstannyl platinum(II) [$Ph_2P(o\text{-}C_6H_4CH_2)Pt(SnMe_3)(PPh_3)$], (5)

Using the same procedure for synthesis of **4**, complex **5** was prepared from ligand **2** (45 mg, 0.10 mmol) and [$Pt(PPh_3)_3$] (100 mg, 0.10 mmol) in toluene reflux rendering a white powder after a 48 h reflux. Isolated yield 60%. Crystals suitable for X-ray diffraction analysis were grown from a THF/CH_2Cl_2 mixture. Anal. Calcd for $C_{40}H_{40}P_2PtSn\cdot C_4H_8O\cdot CH_2Cl_2$: C, 51.30; H, 4.78. Found: C, 51.41; H, 4.67. ^{1}H NMR (700 MHz, C_6D_6, 298 K) δ: 7.59 (1H, dd), 7.59–7.51 (5H, m), 7.12 (4H, t, $^3J_{1H-1H}$ = 10 Hz), 7.06 (2H, m), 7.01 (1H, t, $^3J_{1H-1H}$ = 7.5 Hz), 6.93–6.87 (11H, m), 6.78 (5H, t, $^3J_{1H-1H}$ = 10 Hz), 4.35 (2H, dd, $^3J_{1H-31P}$ = 5 Hz, $^2J_{1H-195Pt}$ = 55 Hz), 0.27 (9H, d, $^3J_{1H-195Pt}$ = 10 Hz, $^2J_{1H-119Sn}$ = 40 Hz). $^{13}C\{^1H\}$ NMR (125.75 MHz, C_6D_6, 298 K) δ: 161.86 (C_{ipso}, dd, $^1J_{13C-31P}$ = 44 Hz, $^3J_{13C-31P}$ = 3 Hz), 137.1 (C_{ipso}, dd, $^1J_{13C-31P}$ = 45 Hz, $^3J_{13C-31P}$ = 4 Hz, $^2J_{13C-195Pt}$ = 22.8 Hz), 134.9 (CH_{arom}, d, $^2J_{13C-31P}$ = 12 Hz, $^3J_{13C-195Pt}$ = 25 Hz), 134.05 (C_{ipso}, d, $^1J_{13C-31P}$ = 19 Hz), 133.17 (s, $J_{13C-31P}$ = 13 Hz), 129.85 (C–H_{arom}, s), 129.55 (CH_{arom}, s), 128.86–127.96 (CH_{arom}, m), 125.32 (CH_{arom}, d, $^3J_{13C-31P}$ = 6 Hz), 29.14 (CH_2, d, $J_{13C-31P}$ = 84 Hz, $^1J_{13C-195Pt}$ = 509.2 Hz), −6.7 (CH_3, d, $^2J_{13C-31P}$ = 10 Hz, $^2J_{13C-195Pt}$ = 68 Hz) $^{31}P\{^1H\}$ NMR (161.9 MHz, C_6D_6, 298 K) δ: 49.5 (d, $^2J_{31P-31P}$ = 11 Hz, $^2J_{31P-195Pt}$ = 1978 Hz, $^2J_{31P-119Sn}$ = 1729 Hz, $^2J_{31P-117Sn}$ = 1654 Hz), 26.8 (d, $^2J_{31P-31P}$ = 11 Hz, $^2J_{31P-195Pt}$ = 2238.3 Hz, $^2J_{31P-119Sn}$ = 170.3 Hz) $^{119}Sn\{^1H\}$ NMR (186.5 MHz, C_6D_6, 298 K) δ: 71.2 (dd, $^2J_{119Sn-31Pcis}$ = 171.58 Hz, $^2J_{119Sn-31Ptrans}$ = 1729.7 Hz, $^1J_{119Sn-195Pt}$ = 10 944.7 Hz). MS (EI^+) 897 m/z $[M+1]^+$.

Synthesis of κ^2-C,P-[(*o*-benzyl)diphenylphosphine]-κ^2-P,Sn-[(*o*-benzyldiphenylstannyl)diphenylphosphine] platinum(II) [$(Ph_2P\text{-}o\text{-}C_6H_4CH_2)Pt(Ph_2P\text{-}o\text{-}C_6H_4CH_2SnPh_3)$], (6)

Using an analogous procedure to the synthesis of **4** and **5**, complex **6** was prepared from ligand **3** (84 mg, 0.10 mmol) and

[$Pt(PPh_3)_3$] (100 mg, 0.10 mmol) rendering a light yellow powder after a 48 h reflux. Isolated yield 70%. Crystals suitable for X-ray diffraction analysis were grown from a THF/CH_2Cl_2 mixture. Anal. Calcd for $C_{50}H_{42}P_2PtSn{\cdot}C_4H_8O$: C, 59.46; H, 4.62. Found: C, 59.96; H, 4.44. ^{1}H NMR (700 MHz, C_6D_6, 298 K) δ: 7.89 (4H, d, $^3J_{H-H}$ = 7 Hz, $^3J_{^1H-^{119}Sn}$ = 42 Hz sat.), 7.75 (1H, d, $^3J_{H-H}$ = 7 Hz, $J_{^1H-^{119}Sn}$ = 70 Hz sat.), 7.74 (1H, d, $^3J_{H-H}$ = 7 Hz, $J_{^1H-^{119}Sn}$ = 70 Hz sat.), 7.08–6.95 (20H, m), 6.89 (2H, t, $^3J_{H-H}$ = 7 Hz), 6.86 (2H, t, $^3J_{H-H}$ = 7 Hz), 6.79 (4H, t, $^3J_{H-H}$ = 7 Hz), 6.75 (1H, t, $^3J_{H-H}$ = 7 Hz), 6.70 (3H, t, $^3J_{H-H}$ = 7 Hz), 4.52 (2H, dd, $^3J_{H-P}$ = 7 Hz, $^3J_{H-H}$ = 3 Hz, $^2J_{^1H-^{195}Pt}$ = 50 Hz sat., CH_2–Pt), 2.62 (2H, br s, $w_{1/2}$ 21 Hz, Sn–CH_2). $^{13}C\{^1H\}$ NMR (100 MHz, C_6D_6, 298 K) δ: 161.35 (C_{ipso}, dd, $^1J_{^{13}C-^{31}P}$ = 44 Hz, $^2J_{^{13}C-^{195}Pt}$ = 28 Hz sat, $^3J_{^{13}C-^{31}P}$ = 3 Hz), 160.19 (C_{ipso}, dd, $^1J_{^{13}C-^{31}P}$ = 33 Hz, $^3J_{^{13}C-^{31}P}$ = 5 Hz), 149.90 (C_{ipso}, d, $^3J_{^{13}C-^{31}P}$ = 10 Hz), 146.94 (d, $^1J_{^{13}C-^{31}P}$ = 29 Hz, $^2J_{^{13}C-^{195}Pt}$ = 90 Hz sat), 137.96 (pseudot, $^2J_{^{13}C-^{119}Sn}$ = 36 Hz sat, $^4J_{^{13}C-^{31}P}$ = 8 Hz), 137.71 (CH_{arom}, s), 135.24 (CH_{arom}, d, $^2J_{^{13}C-^{31}P}$ = 12 Hz), 134.21 (CH_{arom}, d, $^2J_{^{13}C-^{31}P}$ = 20 Hz), 133.81 (CH_{arom}, d, $^3J_{^{13}C-^{31}P}$ = 12 Hz), 133.13 (C_{ipso}, d, $J_{^{13}C-^{31}P}$ = 23 Hz), 133.02 (CH_{arom}, d, $^3J_{^{13}C-^{31}P}$ = 12 Hz), 132.48 (CH_{arom}, d, $^4J_{^{13}C-^{31}P}$ = 10 Hz), 131.06 (CH_{arom}, d, $^2J_{^{13}C-^{31}P}$ = 18 Hz), 130.46 (C_{ipso}, d, $1J_{^{13}C-^{31}P}$ = 27 Hz), 130.10 (CH_{arom}, s), 129.50 (CH_{arom}, s), 128.85 (4CH_{arom}, s), 128.78 (CH_{arom}, s), 128.49 (CH_{arom}, s), 126.93 (CH_{arom}, s), 125.51 (CH_{arom}, d, $^3J_{^{13}C-^{31}P}$ = 6 Hz) 123.4 (CH_{arom}, d, $^3J_{^{13}C-^{31}P}$ = 9 Hz), 22.0 (Sn–CH_2, pseudot, $^2J_{^{13}C-^{195}Pt}$ = 23 Hz sat, $^1J_{^{13}C-^{119}Sn}$ = 37 Hz sat), 21.6 (Pt–CH_2, d, $^2J_{^{13}C-^{31}P}$ = 81 Hz, $^1J_{^{13}C-^{195}Pt}$ = 488 Hz sat). $^{31}P\{^1H\}$ NMR (161 MHz, C_6D_6, 298 K) δ: 50.41 (d, $^2J_{^{31}P-^{31}P}$ = 13 Hz, $^2J_{^{31}P-^{119}Sn}$ = 1807 Hz sat, $^2J_{^{31}P-^{117}Sn}$ = 1726 Hz sat, $^1J_{^{31}P-^{195}Pt}$ = 2328.1 Hz sat), 16.96 (d, $^2J_{^{31}P-^{31}P}$ = 13 Hz, $^2J_{^{31}P-^{119}Sn}$ = 225 Hz sat, $^2J_{^{31}P-^{117}Sn}$ = 199 Hz sat, $^1J_{^{31}P-^{195}Pt}$ = 1978 Hz sat). $^{119}Sn\{^1H\}$ NMR (149 MHz, C_6D_6, 298 K) δ: 71.2 (dd, $^2J_{^{119}Sn-^{31}P}$*cis* = 214.6 Hz, $^2J_{^{119}Sn-^{31}P}$*trans* = 1805.1 Hz, $^1J_{^{119}Sn-^{195}Pt}$ = 11 923.3 Hz). MS (EI^+) 941 m/z $[M - Ph]^+$.

Computational details

The DFT structures *in vacuo* of ligands **1** and **3**, complexes **4**, **4B**, **6** and **6B** [$Pt(PPh_3)_3$] and PPh_3 (Scheme 2 and Fig. 3) were computed at the B3LYP level of theory in conjunction with 6-31G(d) basis set for C, H and P atoms. The platinum and tin atoms were treated with their Stuttgart–Köln 18-active and 4-active electrons relativistic effective core potentials (RECP) in combination with their adapted valence basis sets,[56] respectively. The vacuum-optimized geometries were used as starting points for further optimizations in toluene as solvent using the Polarizable Continuum Model (PCM)[57] as implemented in the Gaussian09 suite of programs.[58] All the optimized structures have been confirmed to be minima through vibrational analysis by the absence of imaginary frequencies and the enthalpies and Gibbs free energies have been obtained using the harmonic approximation at 298 K. Natural Bond Orbital (NBO) analyses[59] were performed on the optimized structures to gain insight into the Sn–Pt bond.

X-ray single crystal diffraction

Crystals of **1–6** were fixed in a glass fibre and measured at 100 K. X-ray intensity data were collected using the program CrysAlisPro on a four-circle SuperNova, Dual EosS2 CCD diffractometer with monochromatic Mo-Kα radiation (λ = 0.71073 Å). Cell refinement, data reduction, incident beam, decay and absorption corrections were carried out with the use of the program CrysAlisPro. Using Olex 2, the structure was solved by direct methods with the program SHELXT and refined by full-matrix least-squares techniques with SHELXL.[62–64] Further details of experimental and structure analyses are given in CCDC 1909928–1909933,‡ respectively. All hydrogen atoms were generated in calculated positions and constrained with the use of a riding model. The final model involved anisotropic displacement parameters for all non-hydrogen atoms.

Conclusions

In conclusion, extension of our methodology for the synthesis of bifunctional silylphosphines allowed efficient access to stannylphosphines bearing methyl or phenyl substituents on Sn. Their reactivity towards [$Pt(PPh_3)_3$] led to isolation of compounds resulting from cyclometallation of the benzylic carbon at the expense of the integrity of the ligand. However, the SnR_3 fragment coordinates forming a heterobimetallic Pt–Sn apolar bond where the Sn moiety essentially coordinates as an X ligand. The $^1J(^{31}P,^{195}Pt)$ values are proposed to indicate a trend in *trans* influence as follows: $SnMe_3$ > $SnPh_2CH_2(o\text{-}C_6H_4)PPh_2$ > $SnPh_3$.

Conflicts of interest

There are no conflicts to declare.

Acknowledgements

This work was supported by CONACyT (CB 242818, PhD grant to JJSD and PD fellowship to ERF), ANR-CONACyT (274001, 253679) and Mississippi State University. We thank Dr Nazario López-Cruz (UAEM) for helpful discussions.

Notes and references

1 A. S. Goldman, A. H. Roy, Z. Huang, R. Ahuja, W. Schinski and M. Brookhart, *Science*, 2006, **312**, 257–261.
2 H. Kameo, Y. Baba, S. Sakaki, D. Bourissou, H. Nakazawa and H. Matsuzaka, *Organometallics*, 2017, **36**, 2096–2106.
3 H. Kameo, S. Ishii and H. Nakazawa, *Organometallics*, 2012, **31**, 2212–2218.
4 L. J. Murphy, M. J. Ferguson, R. McDonald, M. D. Lumsden and L. Turculet, *Organometallics*, 2018, **37**, 4814–4826.
5 B. D. Matson and J. C. Peters, *ACS Catal.*, 2018, **8**, 1448–1455.
6 J. Fajardo and J. C. Peters, *J. Am. Chem. Soc.*, 2017, **139**, 16105–16108.

7 E. Morgan, D. F. MacLean, R. McDonald and L. Turculet, *J. Am. Chem. Soc.*, 2009, **131**, 14234–14236.
8 T. Ogawa, A. J. Ruddy, O. L. Sydora, M. Stradiotto and L. Turculet, *Organometallics*, 2017, **36**, 417–423.
9 L. J. Murphy, H. Hollenhorst, R. McDonald, M. Ferguson, M. D. Lumsden and L. Turculet, *Organometallics*, 2017, **36**, 3709–3720.
10 S. J. Mitton and L. Turculet, *Chem. – Eur. J.*, 2012, **18**, 15258–15262.
11 J. Zamora-Moreno and V. Montiel-Palma, in *Ligand*, ed. C. Saravanan, 2018, Intechopen.
12 M. Simon and F. Breher, *Dalton Trans.*, 2017, **46**, 7976–7997.
13 H. Kameo, T. Kawamoto, D. Bourissou, S. Sakaki and H. Nakazawa, *Organometallics*, 2015, **34**, 1440–1448.
14 H. Kameo, T. Kawamoto, S. Sakaki, D. Bourissou and H. Nakazawa, *Organometallics*, 2014, **33**, 6557–6567.
15 H. Kameo, S. Ishii and H. Nakazawa, *Dalton Trans.*, 2012, **41**, 11386–11392.
16 H. Kameo, S. Ishii and H. Nakazawa, *Dalton Trans.*, 2012, **41**, 8290–8296.
17 H. Kameo and H. Nakazawa, *Chem. Rec.*, 2017, **17**, 268–286.
18 V. Montiel-Palma, O. Piechaczyk, A. Picot, A. Auffrant, L. Vendier, P. Le Floch and S. Sabo-Etienne, *Inorg. Chem.*, 2008, **47**, 8601–8603.
19 V. Montiel-Palma, M. A. Munoz-Hernandez, C. A. Cuevas-Chavez, L. Vendier, M. Grellier and S. Sabo-Etienne, *Inorg. Chem.*, 2013, **52**, 9798–9806.
20 C. A. Cuevas-Chavez, J. Zamora-Moreno, M. A. Munoz-Hernandez, C. Bijani, S. Sabo-Etienne and V. Montiel-Palma, *Organometallics*, 2018, **37**, 720–728.
21 J. Zamora-Moreno, F. Murillo, M. A. Muñoz-Hernández, M. Grellier, S. Pan, S. Jalife, G. Merino, S. Sabo-Etienne and V. Montiel-Palma, *Organometallics*, 2018, **37**, 3581–3587.
22 H. Gilges and U. Schubert, *Eur. J. Inorg. Chem.*, 1998, **1998**, 897–903.
23 M. J. Auburn, R. D. Holmes-Smith and S. R. Stobart, *J. Am. Chem. Soc.*, 1984, **106**, 1314–1318.
24 E. Rufino-Felipe, M. A. Munoz-Hernandez and V. Montiel-Palma, *Molecules*, 2018, **23**, 82.
25 V. Montiel-Palma, M. A. Munoz-Hernandez, T. Ayed, J. C. Barthelat, M. Grellier, L. Vendier and S. Sabo-Etienne, *Chem. Commun.*, 2007, 3963–3965.
26 M. V. Corona-González, J. Zamora-Moreno, C. A. Cuevas-Chávez, E. Rufino-Felipe, E. Mothes-Martin, Y. Coppel, M. A. Muñoz-Hernández, L. Vendier, M. Flores-Alamo, M. Grellier, S. Sabo-Etienne and V. Montiel-Palma, *Dalton Trans.*, 2017, **46**, 8827–8838.
27 H. Weichmann, J. Meunier-Piret and M. van Meerssche, *J. Organomet. Chem.*, 1986, **309**, 267–272.
28 T.-P. Lin, P. Gualco, S. Ladeira, A. Amgoune, D. Bourissou and F. P. Gabbaï, *C. R. Chim.*, 2010, **13**, 1168–1172.
29 H. Kameo, T. Kawamoto, S. Sakaki and H. Nakazawa, *Organometallics*, 2014, **33**, 5960–5963.
30 H. Weichmann, *J. Organomet. Chem.*, 1984, **262**, 279–292.
31 T.-P. Lin and F. P. Gabbaï, *Polyhedron*, 2017, **125**, 18–25.
32 S. Hoppe, H. Weichmann, K. Jurkschat, C. Schneider-Koglin and M. Dräger, *J. Organomet. Chem.*, 1995, **505**, 63–72.
33 S. S. Batsanov, *Inorg. Mater.*, 2001, **37**, 871–885.
34 P. Pyykkö and M. Atsumi, *Chem. – Eur. J.*, 2009, **15**, 186–197.
35 H. Kameo, H. Nakazawa and R. H. Herber, *J. Mol. Struct.*, 2013, **1054–1055**, 321–325.
36 R. A. Gossage, G. D. McLennan and S. R. Stobart, *Inorg. Chem.*, 1996, **35**, 1729–1732.
37 Y.-X. Jia, X.-Y. Yang, W. S. Tay, Y. Li, S. A. Pullarkat, K. Xu, H. Hirao and P.-H. Leung, *Dalton Trans.*, 2016, **45**, 2095–2101.
38 A. Nicolaides, J. M. Smith, A. Kumar, D. M. Barnhart and W. T. Borden, *Organometallics*, 1995, **14**, 3475–3485.
39 T. Marx, L. Wesemann and S. Dehnen, *Organometallics*, 2000, **19**, 4653–4656.
40 E. Wächtler, R. Gericke, E. Brendler, B. Gerke, T. Langer, R. Pöttgen, L. Zhechkov, T. Heine and J. Wagler, *Dalton Trans.*, 2016, **45**, 14252–14264.
41 R. D. Adams, B. Captain and L. Zhu, *Organometallics*, 2006, **25**, 2049–2054.
42 T. G. Appleton, H. C. Clark and L. E. Manzer, *Coord. Chem. Rev.*, 1973, **10**, 335–422.
43 L. Rigamonti, A. Forni, M. Manassero, C. Manassero and A. Pasini, *Inorg. Chem.*, 2010, **49**, 123–135.
44 R. Cervantes, J. Tiburcio and H. Torrens, *New J. Chem.*, 2015, **39**, 631–638.
45 J. Zhu, Z. Lin and T. B. Marder, *Inorg. Chem.*, 2005, **44**, 9384–9390.
46 L. A. Latif, C. Eaborn, A. P. Pidcock and N. S. Weng, *J. Organomet. Chem.*, 1994, **474**, 217–221.
47 T. A. K. Al-Allaf, *J. Organomet. Chem.*, 1999, **590**, 25–35.
48 U. Baltensperger, J. R. Guenter, S. Kaegi, G. Kahr and W. Marty, *Organometallics*, 1983, **2**, 571–578.
49 E. Wächtler, S. Wahlicht, S. H. Privér, M. A. Bennett, B. Gerke, R. Pöttgen, E. Brendler, R. Gericke, J. Wagler and S. K. Bhargava, *Inorg. Chem.*, 2017, **56**, 5316–5327.
50 L.-F. Tang, J. Hong and Z.-K. Wen, *Organometallics*, 2005, **24**, 4451–4453.
51 Z.-K. Wen, Y.-F. Xie, S.-B. Zhao, R.-Y. Tan and L.-F. Tang, *J. Organomet. Chem.*, 2008, **693**, 1359–1366.
52 M. Montag, I. Efremenko, Y. Diskin-Posner, Y. Ben-David, J. M. L. Martin and D. Milstein, *Organometallics*, 2012, **31**, 505–512.
53 M. Gandelman, A. Vigalok, L. Konstantinovski and D. Milstein, *J. Am. Chem. Soc.*, 2000, **122**, 9848–9849.
54 E. G. Bowes, S. Pal and J. A. Love, *J. Am. Chem. Soc.*, 2015, **137**, 16004–16007.
55 S. J. Mitton, R. McDonald and L. Turculet, *Angew. Chem., Int. Ed.*, 2009, **48**, 8568–8571.
56 J. Takaya and N. Iwasawa, *Organometallics*, 2009, **28**, 6636–6638.
57 H. Kameo, S. Ishii and H. Nakazawa, *Dalton Trans.*, 2013, **42**, 4663–4669.
58 M. Albrecht, *Chem. Rev.*, 2010, **110**, 576–623.

59 R. D. Hancock and L. J. Bartolotti, *Polyhedron*, 2013, **52**, 284–293.
60 G. A. Olah, S. Kobayashi and M. Tashiro, *J. Am. Chem. Soc.*, 1972, **94**, 7448–7461.
61 J. Choudhury, S. Podder and S. Roy, *J. Am. Chem. Soc.*, 2005, **127**, 6162–6163.
62 G. M. Sheldrick, *Acta Crystallogr., Sect. C: Struct. Chem.*, 2015, **71**, 3–8.
63 G. M. Sheldrick, *Acta Crystallogr., Sect. A: Found. Adv.*, 2015, **71**, 3–8.
64 O. V. Dolomanov, L. J. Bourhis, R. J. Gildea, J. A. K. Howard and H. Puschmann, *J. Appl. Crystallogr.*, 2009, **42**, 339–341.